The Seventh Asian-Pacific Symposium on Structural Reliability and Its Applications (APSSRA2020)
October 4–7 2020, Tokyo, Japan
T. Takada, I. Yoshida & T. Itoi (editors)

Effects of truncation on transport parameters estimated from spatial and temporal moments in homogeneous porous media

T. Kurasawa[1], M. Suzuki[2] and K. Inoue[3]

[1] *Graduate School of Agricultural Science, Kobe University. Email: 178a052a@stu.kobe-u.ac.jp*
[2] *Graduate School of Agricultural Science, Kobe University. Email: msuzuki@peridot.kobe-u.ac.jp*
[3] *Graduate School of Agricultural Science, Kobe University. Email: mornel@kobe-u.ac.jp*

Abstract: Slug tracer tests can be used to determinate solute transport parameters including the pore velocity and the dispersivity in laboratories and fields. These tests designed to estimate the transport parameters are often based upon the interpretation of spatial moments on spatial concentration distributions (SCDs) or temporal moments of breakthrough curves (BTCs) obtained at fixed locations. In practice, observed SCDs and BTCs are almost exclusively truncated, often because of detection-limit constraint. The purpose of this study is to evaluate effects of truncation on the pore velocity and the longitudinal dispersivity estimates. Specifically, we focus on investigating time- and scale-dependence of the transport parameters estimated from spatial moments of truncated SCDs and temporal moments of truncated BTCs. The results show longitudinal dispersivities from truncated SCDs and BTCs exhibit time- and scale-dependence, respectively. At small distance from injection point, estimating longitudinal dispersivity from temporal moment approach yields erroneous estimates, because BTCs close to the source are significantly non-Gaussian. Pore velocity from spatial moments of truncated SCDs does not depend on time, while that from temporal moments of truncated BTCs depends on distance from injection point.
Keywords: truncation, solute transport parameter, porous media, spatial moment, temporal moment.

1. Introduction

Transport parameters including the pore velocity and the dispersivity are very important to investigate fate and transport of contaminants in natural soils and aquifers. Slug (instantaneous injection) tracer tests can be used effectively to determinate these parameters in laboratories (Fernàndez-Garcia et al. 2004, Berkowitz et al. 2009, Inoue et al. 2016a, Liang et al. 2018) and fields (Sudicky 1986, LeBlanc et al. 1991, Adams and Gelhar 1992). Slug tracer tests designed to estimate transport parameters are often based upon the interpretation of spatial moments on spatial concentration distributions (SCDs) or temporal moments of breakthrough curves (BTCs) obtained at fixed locations (Inoue et al. 2016b, Liang et al. 2018, Zhang et al. 2019). In practice, unfortunately, observed data sets are almost exclusively truncated, often because of detection-limit constraint, i.e., when the tracer concentration is below the limit of detection of the instrument (Young and Ball 2000, Luo et al. 2006, Drummond et al. 2012). In this case, only the tracer concentrations above the limits are detected. Thus, inferring transport parameters from the moments of truncated SCDs and BTCs may yield erroneous estimates. The hydrodynamic dispersion in homogeneous porous media leads to spreading of a tracer plume along longitudinal direction and the average concentrations of SCDs and BTCs decrease with time and distance from injection point, respectively (Bear 1972). Therefore, estimates of the pore velocity and the dispersivity as well as the unmeasured mass due to truncation may be dependent on time and distance from injection point.

Effects of truncation on solute transport parameter estimates have long been recognized. Most studies presented that truncation of tailing edge of BTCs may significantly influence estimates of retardation factors determined from column experiments by the method of moments (Heyse et al. 1997, Young and Ball 2000). However, there are few reports in the literature on the time- and scale-dependence of parameters estimated from truncated data sets.

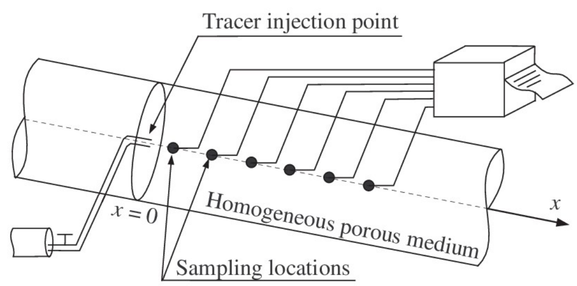

Figure 1. Illustration of slug tracer test. The flow is along the x-axis with a uniform velocity. The boundaries are at $x = \pm\infty$, and will not affect the tracer test results. A slug of conservative tracers instantaneously is injected at $x = 0$.

The purpose of this study is to evaluate the effects of truncation on the pore velocity and the dispersivity estimates. In particular, this paper focuses on investigating time- and scale-dependence of the transport parameters estimated from spatial moments of truncated SCDs and temporal moments of truncated BTCs. An analytical solution was used to generate commonly observed forms of SCDs and BTCs. Then, the generated SCDs and BTCs were artificially truncated. We estimated transport parameters from moments of truncated SCDs and BTCs, and evaluated the effects of truncation on parameter estimation using moment methods.

2. Methodology

2.1 Analytical solution

As illustrated in Fig. 1., let us now consider a slug of solute tracer that is instantaneously injected into a system

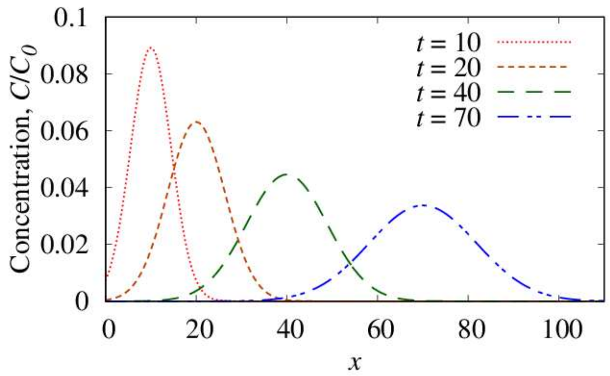

Figure 2. Spatial concentration distributions (SCDs) at various times (t = 10, 20, 40, 70). The shapes of SCDs are Gaussian.

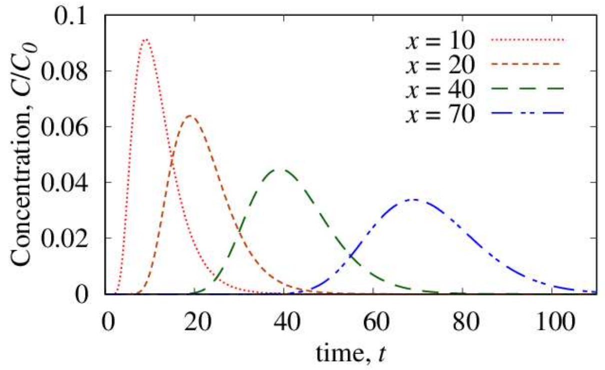

Figure 3. Breakthrough curves (BTCs) at various distances from injection point (x = 10, 20, 40, 70). The shapes of BTCs are non-Gaussian (weakly skew).

governed by 1-D uniform flow along the x-axis. The boundaries are at $x = \pm\infty$, and will not affect the tracer test results. An analytical solution for a slug of conservative tracers instantaneously injected at $x = 0$ can be written as follows (Bear 1972, Sauty 1980, Liang et al. 2018)

$$C(x,t) = \frac{C_0}{\sqrt{4D_L \pi t}} \exp\left(-\frac{(x-\bar{x})^2}{4D_L t}\right) \tag{1}$$

where C is the solute concentration (M/L^3), t is the time (T), C_0 is the solute concentration at $t = 0$ (M/L^3), $D_L = \alpha_L|u| + D_0$ is the longitudinal dispersion coefficient (L^2/T), α_L is the longitudinal dispersivity (L), u is the pore velocity and is along the x-axis (L/T), D_0 is the effective molecular diffusion coefficient in porous media (L^2/T), $\bar{x} = ut$ is the average solute transport distance (L). Unless the pore velocity is extremely small, the effective molecular diffusion coefficient is negligible. In our study, the molecular diffusion is assumed to be negligible ($D_0 =$ 0).

SCDs at various times and BTCs at various sampling locations were obtained based on Eq. (1). In this study, assume $C_0 = 1$ (M/L^3), $\alpha_L = 1$ (L) and $u = 1$ (L/T). The evolutions of SCDs and BTCs are depicted in Fig. 2.

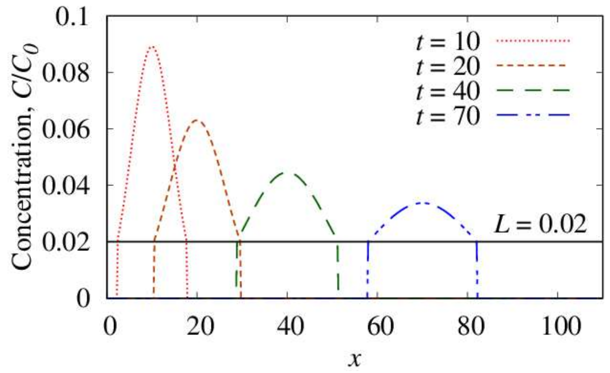

Figure 4. Truncated spatial concentration distributions (SCDs) at various times. The solid line represents the detection limit (L = 0.02). The unmeasured portions in the backward and forward tails of SCDs increase with t

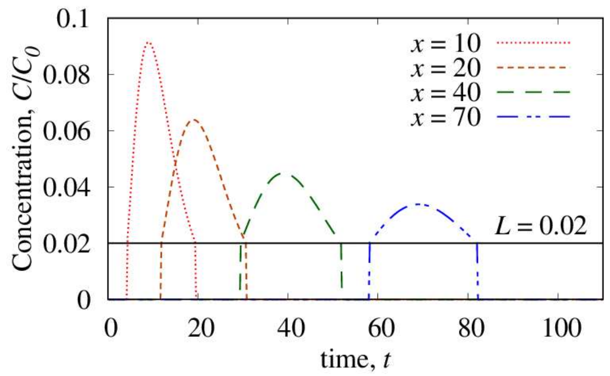

Figure 5. Truncated breakthrough curves (BTCs) at various distances from injection point. The solid line represents the detection limit (L = 0.02). The unmeasured portions in the late time and early time tails of BTCs increase with x.

and Fig. 3., respectively. These figures illustrate the maximum tracer concentrations decay with increasing t and x. Note that the shapes of SCDs (Gaussian) are not consistent with those of BTCs (weakly skew).

2.2 Truncated SCDs and BTCs

A truncated distribution, C_{tr}, is one where data are unavailable below the detection limit L (M/L^3). C_{tr} is can be expressed as

$$C_{tr}(x,t) = \begin{cases} C(x,t) & C(x,t) \geq L \\ 0 & otherwise \end{cases} \tag{2}$$

Complete distribution is thus the special case with $L = 0$. Fig. 4. and Fig. 5. show the truncated SCDs at various times (t = 10, 20, 40, 70) and BTCs at various distances from injection location (x = 10, 20, 40, 70) with L = 0.02 (M/L^3), respectively. It should be noted that the unmeasured portions in the backward and forward tails of SCDs increase with t and those in the late time and early time tails of BTCs increase with x. It is also seen that SCDs are truncated symmetrically, whereas BTCs are truncated asymmetrically.

2.3 Spatial moment approach

The spatial moments of SCDs provide an appropriate means for evaluating the advective and dispersive characteristics of tracer plumes migrating in porous media (Freyberg 1986, Sudicky 1986). The *i*th spatial moment M_i of truncated SCDs obtained at time t is defined as (Freyberg 1986):

$$M_i(t) = \int_{-\infty}^{\infty} C_{tr}(x,t)x^i dx \tag{3}$$

The parameters from truncated SCDs are calculated using the following expressions:

$$M_m = M_0 \tag{4}$$

$$x_{G,tr} = \frac{M_1}{M_0} \tag{5}$$

$$u_{tr} = \frac{x_{G,tr}}{t} \tag{6}$$

$$\alpha_{L,tr} = \frac{\frac{M_2}{M_0} - \left(\frac{M_1}{M_0}\right)^2}{2x_{G,tr}} \tag{7}$$

where M_m is the total mass of the tracer that is above the detection limits (M), $x_{G,tr}$ is the average position of plume in the *x* direction (L), u_{tr} is the pore velocity in the longitudinal direction (L/T) and $\alpha_{L,tr}$ is the longitudinal dispersivity (L).

2.4 Temporal moment approach

The *j*th normalized absolute temporal moments, μ'_j, and the *j*th central temporal moments around the mean, μ_j, are useful descriptors of BTCs; μ'_1 corresponds to the mean arrival time, whereas μ_2 is associated with longitudinal dispersivity (Fernàndez-Garcia et al. 2002, 2004, Inoue et al. 2016a)

$$\mu'_j = \frac{\int_0^{\infty} t^j C_{tr}(x,t)dt}{\int_0^{\infty} C_{tr}(x,t)dt} \tag{8}$$

$$\mu_j = \frac{\int_0^{\infty} (t-\mu'_1)^j C_{tr}(x,t)dt}{\int_0^{\infty} C_{tr}(x,t)dt} \tag{9}$$

Using Eq. (8). and (9)., the pore velocity and the longitudinal dispersivity from truncated BTCs are can be calculated as follows,

$$u_{tr} = \frac{x}{\mu'_1} \tag{10}$$

$$\alpha_{L,tr} = \frac{x}{2}\frac{\mu_2}{(\mu'_1)^2} \tag{11}$$

The total mass of the tracer that is above the detection limits M_m is also computed as

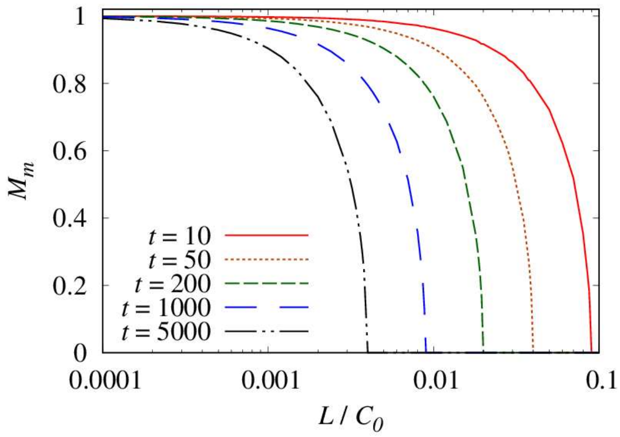

Figure 6. The total mass of the tracer M_m estimated from the spatial moments of SCDs as a function of dimensionless detection limit L/C_0 for different times (*t* = 10, 50, 200, 1000, 5000).

$$M_m = \int_0^{\infty} C_{tr}(x,t)dt \tag{12}$$

3. Results and discussion

3.1 Parameters estimated from SCDs

Fig. 6. shows the total mass of the tracer M_m estimated from the spatial moments of truncated SCDs as a function of dimensionless detection limit L/C_0 for different times (t = 10, 50, 200, 1000, 5000). For all times, as dimensionless detection limit approaches zero, M_m approaches the complete data set value ($M_m = 1$) and relative error between truncated and complete data set values approaches zero. It can be also seen that M_m decays exponentially with increasing L/C_0 and converges to zero. This result demonstrates that the effect of detection limit is more pronounced at large detection limit. Fig. 6. also shows as the time t increases, the total mass of the tracer M_m is significantly underestimated. As expected, we find that the unmeasured mass due to truncation is dependent on time.

Fig. 7. presents the average position of plume in the *x* direction $x_{G,tr}$ with dimensionless detection limit L/C_0. The results show that $x_{G,tr}$ remains constant for all times and are attributed to symmetrical truncation of SCDs (Gaussian). As a result, pore velocity u_{tr} estimated from spatial moments of truncated SCDs is not also dependent on time.

Fig. 8. shows dimensionless longitudinal dispersivity $\alpha_{L,tr}/\alpha_L$ as a function of dimensionless detection limit L/C_0. Similar to the total mass of the tracer (Fig. 6.), $\alpha_{L,tr}/\alpha_L$ decays exponentially with increasing L/C_0 and converges to zero. This result suggests that the unmeasured mass in the SCDs due to truncation leads to underestimation of $\alpha_{L,tr}/\alpha_L$. For instance, at $t = 1000$ and 5000, when the dimensionless detection limit L/C_0 is 0.01, the dimensionless longitudinal dispersivity $\alpha_{L,tr}/\alpha_L$ is 0. Also, the time-dependence of longitudinal dispersivity estimates from temporal moments of truncated

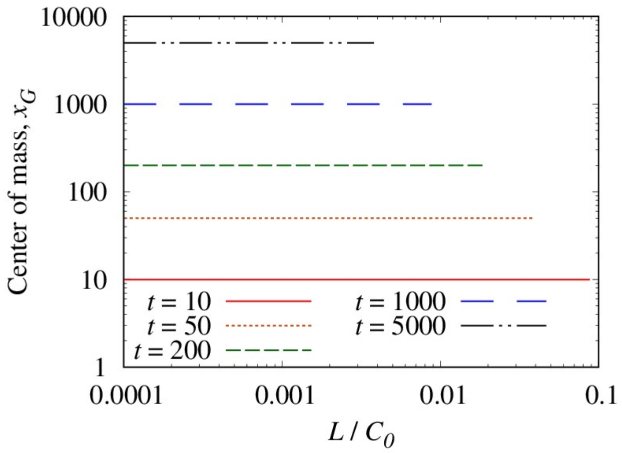

Figure 7. The average positions of plume in the x direction $x_{G,tr}$ estimated from the spatial moments of SCDs as a function of dimensionless detection limit L/C_0 for different times (t = 10, 50, 200, 1000, 5000). $x_{G,tr}$ remains constant for all times.

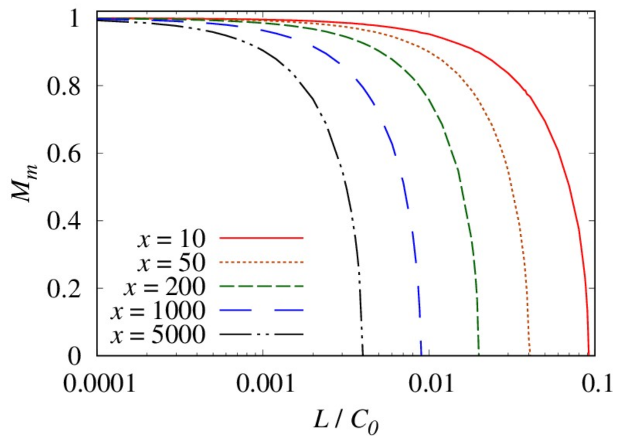

Figure 9. The total mass of the tracer M_m estimated from the temporal moments of BTCs as a function of dimensionless detection limit L/C_0 for different distances from injection point (x = 10, 50, 200, 1000, 5000).

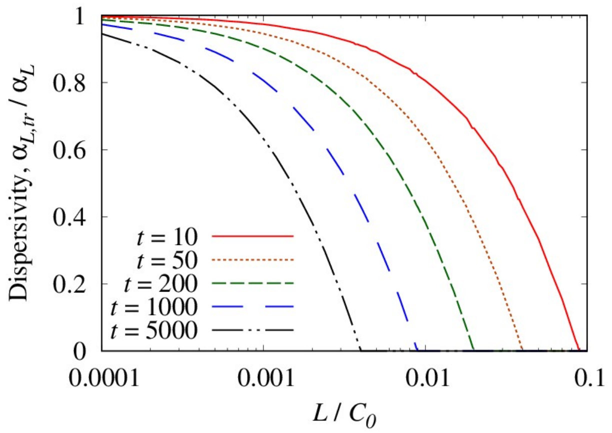

Figure 8. The dimensionless longitudinal dispersivity $\alpha_{L,tr}/\alpha_L$ estimated from the spatial moments of SCDs as a function of dimensionless detection limit L/C_0 for different times (t = 10, 50, 200, 1000, 5000).

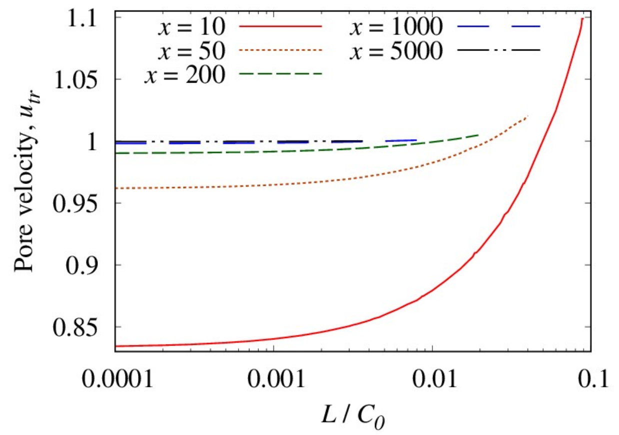

Figure 10. The pore velocity u_{tr} estimated from the temporal moments of BTCs as a function of dimensionless detection limit L/C_0 for different distances from injection point (x = 10, 50, 200, 1000, 5000).

SCDs is illustrated in Fig. 8..

3.2 Parameters estimated from BTCs

Fig. 9. and Fig. 10. show the total mass of the tracer M_m and the pore velocity u_{tr} estimated from temporal moments of truncated BTCs as a function of dimensionless detection limit L/C_0 for different distances from injection point (x = 10, 50, 200, 1000, 5000), respectively. The truncation effect of M_m estimated from BTCs is very similar to that estimated from SCDs, whereas there is the difference in truncation effects between pore velocities estimated from spatial (SCDs) versus temporal (BTCs) moments. At small truncation limit, the unmeasured portions in the early time tails of BTCs are smaller than those in the late time tails, because BTCs are positively skewed (non-Gaussian). Thus, at small dimensionless detection limit L/C_0, pore velocity estimated from truncated BTCs is underestimated. It should be noted that at a small distance from injection point, this effect is more pronounced due to strong skewness. For the large truncation limit, truncation overestimates pore velocity. These results show that truncation of BTCs leads to both over- and underestimation of pore velocity.

Longitudinal dispersivities estimated from temporal moments of truncated BTCs are presented in Fig. 11.. This figure shows longitudinal dispersivity from truncated BTCs exhibit scale-dependence (except for $x = 10$), whereas at small detection limit L/C_0 and for $x = 10$, dimensionless longitudinal dispersivity does not exhibit scale-dependence. Because BTCs close to the source are significantly non-Gaussian, at small distance from injection point, estimating longitudinal dispersivity from

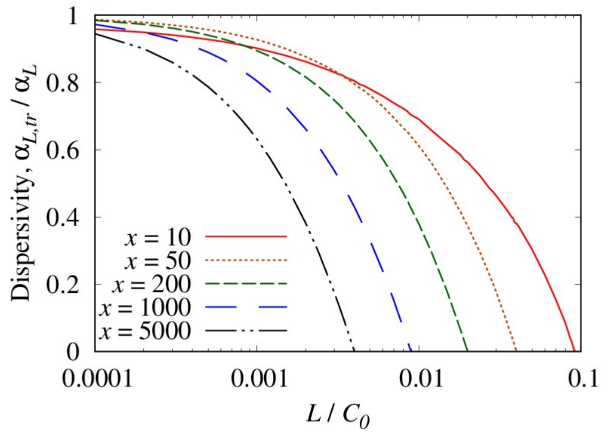

Figure 11. The dimensionless longitudinal dispersivity $\alpha_{L,tr}/\alpha_L$ estimated from the temporal moments of BTCs as a function of dimensionless detection limit L/C_0 for different distances from injection point (x = 10, 50, 200, 1000, 5000).

Eq. (11)., which assumes Gaussian distribution, yields erroneous estimates.

4. Conclusions

In this study, the effects of truncation on transport parameters including pore velocity and longitudinal dispersivity estimated from spatial moments of spatial concentration distributions (SCDs) and temporal moments of breakthrough curves (BTCs) were evaluated. We used an analytical solution to generate commonly observed forms of SCDs and BTCs in order to analyze the effects of truncation. The main conclusions from this study are summarized as follows:

1. The unmeasured portions in the SCDs and BTCs due to truncation lead to underestimation of longitudinal dispersivities estimated from spatial and temporal moments.
2. Longitudinal dispersivities estimated from truncated SCDs and BTCs exhibit the time- and scale-dependence, respectively.
3. Pore velocity from spatial moments of SCDs does not depend on time, whereas that from temporal moments of BTCs depends on distance from injection point. This is because the shapes of BTCs are non-Gaussian.
4. Because BTCs close to the source are significantly non-Gaussian, at small distance from injection point, estimating longitudinal dispersivity from temporal moment approach yields erroneous estimates.

It should be noted that these conclusions may not be extended directly to laboratory and field experiments, since our study focused on one-dimensional homogeneous porous media. Ongoing work is aimed at developing different experimental conditions, including two- and three-dimensional groundwater flow and heterogeneous porous media.

Acknowledgments

This work was supported by JSPS KAKENHI Grant Numbers JP19H03074, JP20J10801.

References

Adams, E.E. and Gelhar, L.W. 1992. Field study of dispersion in a heterogeneous aquifer: 2. Spatial moment analysis. Water Resources Research, 28(12): 3293-3307.

Bear, J. 1972. Dynamics of fluids in porous media. Dover Publications: 764p..

Berkowitz, B., Cortis, A., Dror, I. and Scher, H. 2009. Laboratory experiments on dispersive transport across interfaces: The role of flow direction. Water Resources Research, 45:W02201.

Drummond, J.D., Covino, T.P., Aubeneau, A.F., Leong, D., Patil, S., Schumer, R. and Packman, A.I. 2012. Effects of solute breakthrough curve tail truncation on residence time estimates: A synthesis of solute tracer injection studies. Journal of Geophysical Research, 117: G00N08.

Fernàndez-Garcia, D., Sánchez-Vila, X. and Illangasekare, T.H. 2002. Convergent-flow tracer tests in heterogeneous media: combined experimental-numerical analysis for determination of equivalent transport parameters. Journal of Contaminant Hydrology, 57: 129-145.

Fernàndez-Garcia, D., Illangasekare, T.H. and Rajaram, H. 2004. Conservative and sorptive forced-gradient and uniform flow tracer tests in a three-dimensional laboratory test aquifer. Water Resources Research, 40: W10103.

Freyberg, D.L. 1986. A natural gradient experiment on solute transport in a sand aquifer: 2. Spatial moments and the advection and dispersion of nonreactive tracers. Water Resources Research, 22(13): 2031-2046.

Heyse, E., Dai, D., Rao, P.S.C. and Delfino, J.J. 1997. Development of a continuously stirred flow cell for investigating sorption mass transfer. Journal of Contaminant Hydrology, 25: 337-355.

Inoue, K., Kurasawa, T. and Tanaka, T. 2016a. Quantification of macrodipsersion in laboratory-scale heterogeneous porous formations. International Journal of GEOMATE, 10(21): 1854-1861.

Inoue, K., Kurasawa, T. and Tanaka, T. 2016b. Spatial and temporal moment approaches to quantify laboratory-scale macrodispersion in stratified porous formations, Journal of Rainwater Catchment Systems, 22(1): 15-22.

LeBlanc, D.R., Garabedian, S.P., Hess, K.M., Gelhar, L.W., Quadri, R.D., Stollenwerk, K.G. and Wood, W.W. 1991. Large-scale natural gradient tracer test in sand and gravel, Cape Cod, Massachusetts 1. Experimental design and observed tracer movement. Water Resources Research, 27(5): 895-910.

Liang, X., Zhan, H., Liu, J., Dong, G. and Zhang, Y. 2018. A simple method of transport parameter estimation for slug injecting tracer tests in porous media. Science of the Total Environment, 644: 1536-1546.

Luo, J., Cirpka, O.A. and Kitanidis, P.K. 2006. Temporal-moment matching for truncated breakthrough curves for step or step-pulse injection. Advances in Water Resources, 29: 1306-1313.

Sauty, J.P. 1980. An analysis of hydrodispersive transfer in aquifers. Water Resources Research, 16(1): 145-158.

Sudicky, E.A. 1986. A natural gradient experiment on solute transport in a sand aquifer: Spatial variability of hydraulic conductivity and its role in the dispersion process. Water Resources Research, 22(13): 2069-2082.

Young, D.F. and Ball, D.F. 2000. Column experimental design requirements for estimating model parameters from temporal moments under nonequilibrium conditions. Advances in Water Resources, 23: 449-460.

Zhang, C., Suekane, T., Minokawa, K., Hu, Y. and Patmonoaji, A. 2019. Solute transport in porous media studied by lattice Boltzmann simulations at pore scale and x-ray tomography experiments. Physical Review E, 100: 063110.